2017-04-28

# Implications of SAR ambiguities in estimating the motion of slow targets

Garren, David A.

Garren, David A. "Implications of SAR ambiguities in estimating the motion of slow targets." In Algorithms for Synthetic Aperture Radar Imagery XXIV, vol. 10201, p. 102010E. International Society for Optics and Photonics, 2017.
http://hdl.handle.net/10945/59220

# Implications of SAR ambiguities in estimating the motion of slow targets

David A. Garren

David A. Garren, "Implications of SAR ambiguities in estimating the motion of slow targets," Proc. SPIE 10201, Algorithms for Synthetic Aperture Radar Imagery XXIV, 102010E (28 April 2017); doi: 10.1117/12.2263096

Event: SPIE Defense + Security, 2017, Anaheim, California, United States

# Implications of SAR Ambiguities in Estimating the Motion of Slow Targets

David A. Garren

Naval Postgraduate School, Monterey, California, USA

## ABSTRACT

This paper examines the implications pertaining to the problem of attempting to invert synthetic aperture radar (SAR) measurement data to yield unique estimates of the underlying motion of slow targets in the imaged scene. A recent analysis has demonstrated that ambiguities exist in estimating the kinematics parameters of surface targets for general bistatic SAR collection data. In particular, a procedure has been developed which generates alternate target trajectories which give the same SAR measurements as that of the true target motion. The current paper extends the earlier analysis by generating specific numeric examples of alternate target trajectories corresponding to the motion of a given slowly moving target. This slow-target case reveals the counter-intuitive result that a single SAR collection data set can be generated by target trajectories with significantly different, and possibly opposing, heading directions. For example, the true motion of a given target can be moving towards the mean radar position during the SAR collection interval, whereas a valid alternate trajectory can correspond to a target that is moving away from the radar. The present analysis demonstrates the extent of the challenges associated with attempting to estimate of the underlying motion of targets using SAR measurement data.

**Keywords:** Synthetic aperture radar, Radar theory, Moving Targets

## 1. INTRODUCTION

SAR processing can produce remarking remarkable imaging quality of stationary objects and terrain. However, moving targets typically yield artifacts in SAR imagery, which are often smeared beyond recognition. A number of researchers have attempted to understand the nature of the motion-induced target smears. One frequent goal is to attempt to refocus[1–22] the smeared artifacts so that the resulting image is similar to that of stationary objects.

There has been research into the general properties of such moving target artifacts.[1–4] In addition, there have also been other investigations of the properties of moving target smears. For example, some researchers have attempted to improve the detection of such targets via the use of focusing methods.[5–17] A number of other investigators considered various methods for detecting moving targets through these signature techniques.[23–28] Finally, these moving target smear have been shown to exhibit curvature in the radar down-range direction.[18, 29–35]

Some investigators[36–40] noticed that ambiguities appear to arise in attempting to estimate target motion parameters corresponding to these smear artifacts. Some of the examples include monostatic collections in which both the radar and target move with constant velocity during the collection of the radar measurements. Specifically, identical phase history data sets are obtained from alternate fictitious target trajectories.

A recent investigation[41] extends the formalism regarding these ambiguities to include completely arbitrary trajectory and speed profiles for the radar transmitter, the radar receiver, and the target. In particular, this work presents the specific equations that can be used to generate alternate fictitious target trajectory and speed profiles which give exactly the same radar measurement data as that corresponding to the true motion of the target. That is, the analysis shows that it is not possible to form unique estimates of target motion of based upon general bistatic radar range measurements. These results apply even if range-rate or doppler measurements are collected as well. This ambiguity can be broken only through the use of additional constraints, such as target motion on the one-dimensional (1D) locus of a road. Therefore, the ability to localize a moving target based

Further author information: (Send correspondence to D.A.G.)
E-mail: dagarren@nps.edu

Algorithms for Synthetic Aperture Radar Imagery XXIV, edited by Edmund Zelnio, Frederick D. Garber,
Proc. of SPIE Vol. 10201, 102010E · © 2017 SPIE · CCC code: 0277-786X/17/$18 · doi: 10.1117/12.2263096

upon general bistatic radar range measurements depends upon the overlap of the transmission and reception mainbeams. Throughout these discussions, the concept of a bistatic radar collection includes the degenerate monostatic case in which the transmitter and receiver are co-located on the same platform.

In the current paper, the special case of a slowly moving target is examined in more detail. In particular, this analysis attempts to generate an alternate target trajectory which is significantly different in terms of the heading direction. A special emphasis is placed on the generation of alternate fictitious targets in which the heading direction is opposite to that of the true target.

## 2. TRUE TRAJECTORY OF SLOW MOVING TARGET

The fundamental result of the previous ambiguity analysis[41] is that a number of differing target trajectory and speed profiles can give the same set of bistatic radar measurements. That is, one cannot use a set of bistatic range measurement data in order to generate an accurate estimate of the underlying target motion. Additional constraints are required, as with the assumption that the target lies along the 1D locus of a road.

A number of definitions are required in order to properly summarize the results of previous ambiguity work.[41] It is assumed that the radar transmitter and receiver are permitted to move with arbitrary trajectories and speed profiles. It is also assumed that the instantaneous positions of the transmitter and receiver can be known with arbitrary precision. The target is permitted with move with an arbitrary trajectory and speed profile on the surface of a ground-plane. However, the target trajectory and speed profile is assumed to be unknown to the radar system. In addition, the speeds of the transmitter, receiver, and target are assumed to be much less than the speed of light, which is consistent with radar collection.

The transmitter is assumed to emanate a total of $N$ radar waveforms during the coherent processing interval of the SAR collection. Define $\tau_{t,n}$ to be the average value of the slow-time corresponding to the $n^{th}$ waveform. Likewise, set $\tau_{r,n}$ to be equal to the average time of waveform absorption by the receiver after scattering off of the target. In addition, the time interval between successive waveforms is not constrained to be fixed and instead is permitted to vary in any manner.

Next, a number of geometrical definitions are required. In general, a three-dimensional (3D) ellipsoid is formed as a 2D ellipse of revolution about the axis connecting the locations of the transmitter at waveform emanation and the receiver at waveform absorption. These transmitter and receiver locations correspond to the two foci of this ellipsoid. Define $\mathbf{x}_{t,n} = \{x_{t,n}, y_{t,n}, z_{t,n}\}$ to be the location of the transmitter phase center corresponding to the transmission time $\tau_{t,n}$. Similarly, define $\mathbf{x}_{r,n} = \{x_{r,n}, y_{r,n}, z_{r,n}\}$ to be the location of the receiver phase center at the reception time $\tau_{r,n}$.

This analysis is generated in terms of a local Cartesian coordinate system in which the $x - y$ plane is tangent to the local surface of the earth. Then, the location of the target at the waveform scattering time $\tau_{s,n}$ is given by $\mathbf{x}_{s,n} = \{x_{s,n}, y_{s,n}, 0\}$.

Define $\Delta f_n$ to be the temporal bandwidth of the radar, wherein the index $n$ denotes the particular waveform within the transmitted sequence during the synthetic aperture. It is assumed that this bandwidth is permitted to be arbitrarily wide. Furthermore, the target is modeled as an idealized point scattering center, so that waveform properties before scattering are preserved when absorbed into the receiver. The actual measurement of the bistatic range of the radar system to the target is denoted by $R_n$. In addition, the permission of an arbitrarily wide waveform bandwidth implies that the bistatic range error $\delta R_n$ can be arbitrarily small as well.

## 3. ALTERNATE TARGET CONSTRUCTION

The bistatic ambiguity analysis[41] continues by generating arbitrary trajectories and speed profiles for the radar transmitter and receiver. In addition, there are $N$ bistatic range measurements of the moving target relative to the radar system. Next, a particular prescription provides a means for computing any number of alternate fictitious target trajectory and speed profiles with yield the same bistatic range measurement values. As clarified in the original development, the location and other motion parameters corresponding to a given alternate target trajectory is not required to lies within some particular small neighborhood about the true target values. Instead, the instantaneous position of the fictitious target trajectory needs only to lie within the overlap of the transmission and reception beampatterns for this waveform. For convenience of notation, this waveform index $n$ is suppressed until later in order to avoid cumbersome mathematical notation.

A few definitions are repeated from the earlier ambiguity analysis[41] for convenience. In this vein, denote the round-trip waveform propagation fast-time via:

$$\Delta\tau \equiv \tau_r - \tau_t = \frac{2R}{c}, \tag{1}$$

which also yields the value of the bistatic range $R$ from the moving target to the radar system. Denote the location of the transmitter phase center at the time of waveform emanation to be $\mathbf{x}_t$, which is expressed in terms of the Cartesian ground-plane coordinate system discussed above. Similarly, denote the location of the receiver phase center at the time of waveform absorption to be $\mathbf{x}_r$. Next, the location of the center of the 3D ellipsoid is given by:

$$\mathbf{x}_0 \equiv \frac{1}{2}\big\{\mathbf{x}_r + \mathbf{x}_t\big\}. \tag{2}$$

Define the actual value of the ellipsoid center to be $\{x, y, z\} = \{X_0, Y_0, Z_0\}$ in terms of the selected ground-plane coordinate system.

The previous analysis[41] defines the vector between the transmitter and receiver to be:

$$\mathbf{w} \equiv \mathbf{x}_r - \mathbf{x}_t. \tag{3}$$

In particular, define the Cartesian components of $\mathbf{w}$ along the ground-plane unit vectors $\{\hat{\mathbf{x}}, \hat{\mathbf{y}}, \hat{\mathbf{z}}\}$ to be given by $\{w_x, w_y, w_z\}$. Next, the elevation $\Phi$ and azimuthal $\Theta$ angles of the 3D ellipsoid relative to the ground-plane coordinates are given by:

$$-\frac{\pi}{2} \leq \Phi \equiv \arctan\left(\frac{w_z}{\sqrt{w_x^2 + w_y^2}}\right) \leq \frac{\pi}{2}, \tag{4}$$

$$-\pi < \Theta \equiv \arctan\left(\frac{w_y}{w_x}\right) \leq \pi. \tag{5}$$

In these equations, the quadrant of $\Theta$ is determined by the signs of the values of $w_x$ and $w_y$. In particular, a value of $\Theta$ between zero and $\pi$ is obtained for positive $w_y$, and an angle that lies between $-\pi$ and zero results from a negative value of $w_y$.

The generation of an alternate fictitious trajectory begins with the selection of a different location than that of the true target at the time for the initial waveform. This initial location is not constrained to lie within some small neighborhood about the true target location, but it is required to lie within the overlap of the transmission and reception energy beampatterns. In addition, this alternate target location is constrained to lie on a 2D ellipse within the ground-plane, which is defined according to the equation:[41]

$$\sum_{0 \leq \alpha + \beta \leq 2} p_{\alpha,\beta}\ x^\alpha y^\beta = 0. \tag{6}$$

In this equation, the values of the $p_{\alpha\beta\gamma}$ are computed via:

$$p_{20} \equiv \rho, \tag{7}$$

$$p_{02} \equiv \omega, \tag{8}$$

$$p_{11} \equiv \{\psi - \eta\}\sin(2\Theta), \tag{9}$$

$$p_{10} \equiv -2X_0\,\rho - Y_0\{\psi - \eta\}\sin(2\Theta) - Z_0\{\xi - \eta\}\cos(\Theta)\sin(2\Phi), \tag{10}$$

$$p_{01} \equiv -X_0\{\psi - \eta\}\sin(2\Theta) - 2Y_0\,\omega - Z_0\{\xi - \eta\}\sin(\Theta)\sin(2\Phi), \tag{11}$$

$$\begin{aligned} p_{00} \equiv &-\frac{1}{4} + X_0^2\,\rho + Y_0^2\,\omega + Z_0^2\,\gamma + X_0Y_0\{\psi - \eta\}\sin(2\Theta) \\ &+ X_0Z_0\{\xi - \eta\}\cos(\Theta)\sin(2\Phi) + Y_0Z_0\{\xi - \eta\}\sin(\Theta)\sin(2\Phi). \end{aligned} \tag{12}$$

These equations also define values for $\xi$, $\eta$, $\psi$, $\gamma$, $\rho$, and $\omega$ according to the following:

$$\xi \equiv \{c\,\Delta\tau\}^{-2}, \tag{13}$$

$$\eta \equiv \left\{\{c\,\Delta\tau\}^2 - \|\mathbf{x}_r - \mathbf{x}_t\|^2\right\}^{-1}, \tag{14}$$

$$\psi \equiv \xi\cos^2(\Phi) + \eta\sin^2(\Phi), \tag{15}$$

$$\gamma \equiv \xi\sin^2(\Phi) + \eta\cos^2(\Phi), \tag{16}$$

$$\rho \equiv \psi\cos^2(\Theta) + \eta\sin^2(\Theta), \tag{17}$$

$$\omega \equiv \psi\sin^2(\Theta) + \eta\cos^2(\Theta). \tag{18}$$

The ellipse equation (6) determines the locus of possible alternate ground-plane scattering locations $\{x, y\}$ of the waveform off of the moving target.

The next step in the processing[41] is to choose an alternate fictitious location within the beampattern overlap for the first scattering event off of the moving target. One possible methodology is based upon the selection of an alternate value for the ground-plane coordinate $x$ with the radar beampattern overlap region. Then, (6) is used to determine the constrained values of the $y$ coordinate via:[41] for the value of $y$:

$$y = \frac{-p_{110}\,x - p_{010} \pm \sqrt{g(x)}}{2\,p_{020}}. \tag{19}$$

Here, the following function is defined:

$$g(x) \equiv \{p_{110}\,x + p_{010}\}^2 - 4\,p_{020}\{p_{200}\,x^2 + p_{100}\,x + p_{000}\}. \tag{20}$$

In order to obtain real-valued solutions for (19), it is necessary to ensure that $g(x)$ is non-negative. In general, the quadratic equation of (19) implies that there exist two possible solutions. Again, it is only necessary to select a solution that lies within the overlap region of the transmission and reception beampatterns.

The previous ambiguity analysis[41] also presents a method for computing the value of the fast-time $\tau$ which is consistent with the alternate target position $\mathbf{x} \equiv \{x, y, z\}$ which is generated using (19). The value of this particular time $\tau$ at which the waveform scatters off of the target is obtained via:

$$\tau = \tau_t + \frac{\ell_t}{c}. \tag{21}$$

In this equation, the value of the path length that the waveform traverses is going from the transmitter to the points of scattering off of the target is obtained via:

$$\ell_t \equiv \|\mathbf{x}_t - \mathbf{x}\|. \tag{22}$$

That is, the alternate fictitious target trajectory which is generated will have, in general, a different value for the time of scattering off of the target relative to that of corresponding to the true target trajectory.

The discussion of the prior ambiguity investigation[41] clarifies that actual value of the scatter time $\tau$ is itself ambiguous, since the radar measures only the total distance traversed by the waveform in going from the transmitter to the target and then into the receiver. However, once a particular set of alternate spatial coordinates $\{x, y, 0\}$ has been generated, then the corresponding value of the scattering time $\tau$ for this fictitious trajectory becomes determined via (21). Note that this ambiguity in the actual scattering time disappears for monostatic collections, since its value can be assumed to be the midpoint between the transmission and reception times.

The discussion above presents a methodology which can used to generate an alternate target location and scattering time $\{x_1, y_1, z_1, \tau_1\}_{\text{alt}}$ which yields the same bistatic range measurement $R_1$ for the initial waveform as that which applies for the true space-time point $\{x_1, y_1, z_1, \tau_1\}_{\text{true}}$. This same procedure applies in generating alternate space-time points $\{x_n, y_n, z_n, \tau_n\}_{\text{alt}}$ corresponding to waveform index $n$ within the SAR collection interval. Here, the waveform index is included again for clarity of presentation. Therefore, the full alternate fictitious target trajectory and speed profile can be generated.

## 4. NUMERIC EXAMPLE OF A SLOW TARGET

This section presents a particular example corresponding to a slowly moving target. This case considers a monostatic SAR collection with a radar that is pointing broadside in the starboard direction. For this example, the radar and target travel with constant velocity.

The radar transmits 1001 waveforms over a 1-second synthetic aperture interval with a pulse repetition frequency (PRF) of 1 kHz. The values for the average location of the radar and the moving target are given by $\{-0, 6, 0.5\}$km and $\{300, 0, 0\}$km, respectively, with regards to the selected coordinates $\{x, y, z\}$, with units of kilometers. The corresponding $\{x, y, z\}$ components of the velocity vector are selected to be $\{200, 0, 0\}$m/s and $\{0.5, -5, 0\}$m/s, respectively, wherein the units are meters per second.

A fictitious target trajectory and speed profile which is consistent with the bistatic range measurements is obtained[41] is obtained by selecting an alternate set of $x$ coordinate values for the target location corresponding to each waveform along the synthetic aperture. A possible methodology involves the scaling and shifting of the true target values of $x$ is order to obtain the corresponding fictitious values. For the particular slow moving target examined herein, a scale of $-1$ and a shift of $-0.6$ km are applied to generate the $x$ coordinate values of the fictitious target for each waveform along the synthetic aperture. Next, these $x$ values are used within (19) to solve for the corresponding $y$ coordinates values for each waveform. Thus, these computation yield values for the fictitious target locations $\{x, y, 0\}$ on the surface of the ground-plane for each transmitted waveform.

The monostatic collection geometry for this particular example is shown in Figure 1. In this figure, the trajectories of the slow target and the generated fictitious target almost appear only as points in this figure. Thus, it is useful to examine an image zooms of the spatial region around both the true and fictitious targets, as is shown in Figure 2 and 3. In both of these figures, the initial 200 ms of the total 1000 ms corresponding to the full synthetic aperture is shown with a solid line is shown with a solid line, and the remainder is given by a dashed line. Thus, the true target is moving away from the radar that lies distant in the $+y$ direction. In contrast, the alternate fictitious target is moving towards the radar in a direction which is approximately opposite to that of the true target motion.

The average speed variation for the alternate fictitious target trajectory is presented in Figure 4. The variation in the fictitious target speed in this figure is only approximately 0.1 sec over the 1 sec SAR processing interval. Likewise, Figure 5 reveals the heading of the fictitious target varies by less than $0.1°$ over the SAR collection interval. These results indicate that the speed and heading variation are very minor, so there would be relatively little stress on the engines and tires if one were to attempt to travel according to this alternate target trajectory and speed profile.

A comparison of the bistatic range values corresponding to the true target motion and that of the alternate fictitious target are presented in Figure 6. This figure shows that the alternate fictitious target yields exactly the same bistatic range profile along the synthetic aperture as that of the true target motion. Detailed examination reveals that the differences between the two profiles lies on the order of computational machine precision.

## 5. CONCLUSIONS

There has been recent work in the understanding of ambiguities in the inferred target trajectory and speed profile based upon the collection of general bistatic range measurements. In particular, specific equations have been developed for computing alternate fictitious target trajectory and speed profiles which yield identical radar measurement data as that obtained from the true target motion. The current paper investigates the special case of a slowly moving target in more detail. A simulation is generated for the case of a monostatic radar collection from a typical SAR collection system which is imaging with broadside geometry. A target is included within the system which is moving approximately in the radar down-range direction away from the radar.

The current study reveals that it is possible to generate an alternate fictitious target trajectory and speed profile corresponding to a target that is moving is approximately the opposite direction as that of the true target motion. This result can appear counter-intuitive initially, but this result arises naturally from the mathematics and can be understood by examining the rotation of the wavefronts at the scene center as the radar platform traverses the full synthetic aperture.

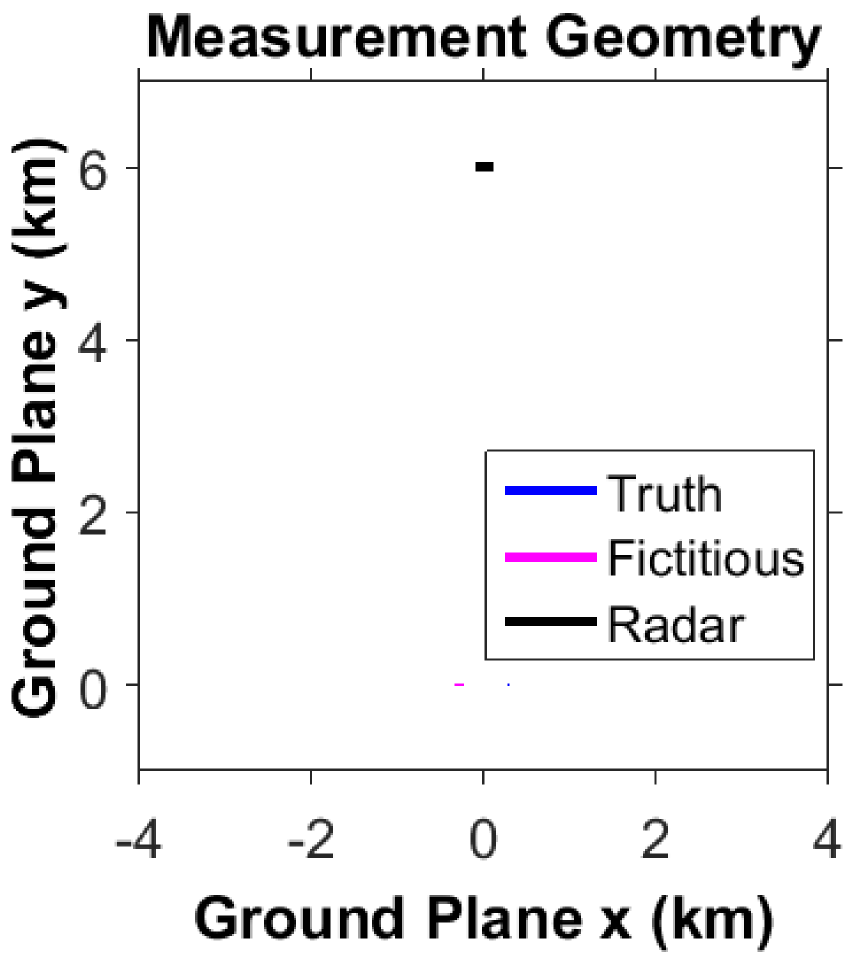


Figure 1. The monostatic collection geometry for this particular example, showing the radar trajectory. The trajectories corresponding to the true and fictitious targets appear approximately as points in the spatial region of $\{x, y\} = \{0, 0\}$ near the lower left of the legend box.

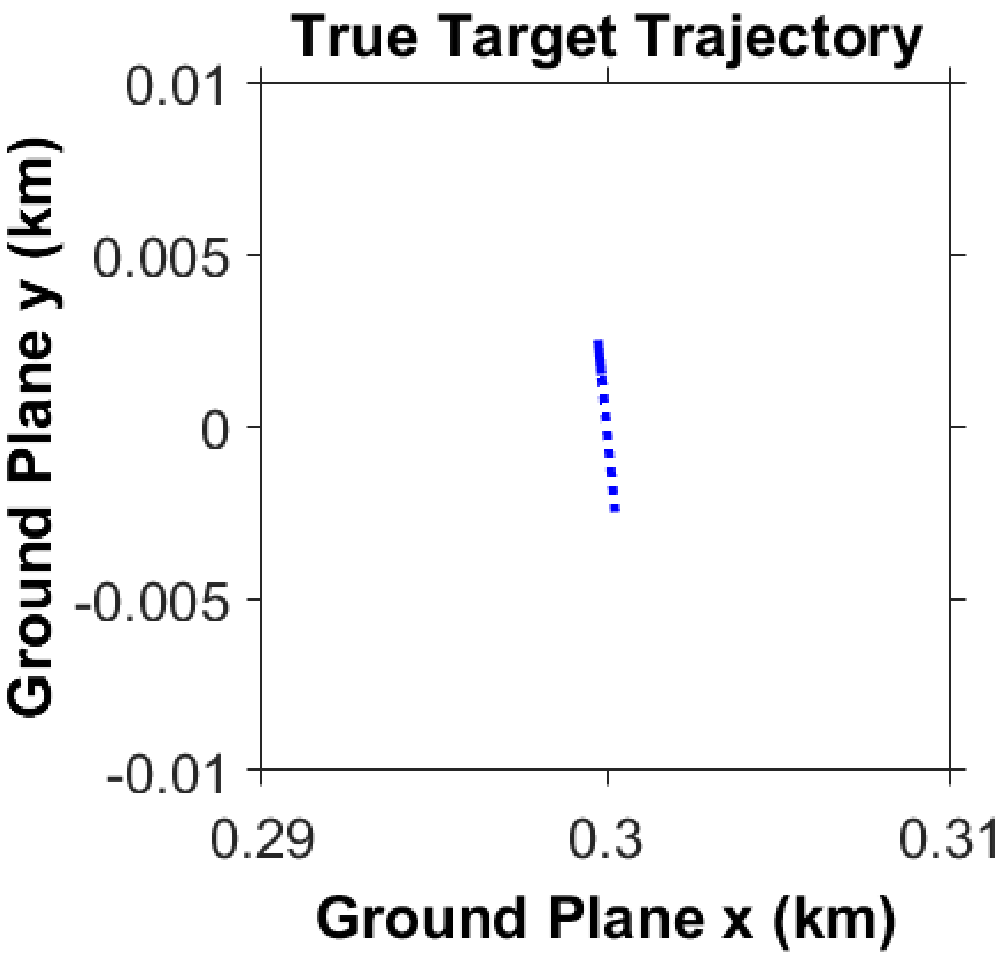


Figure 2. A zoomed image of the true target trajectory, wherein the initial 200 ms of the total 1000 ms corresponding to the full synthetic aperture is shown with a solid line, and the remainder is given by a dashed line. Thus, the true target is moving away from the radar that lies distant in the $+y$ direction.

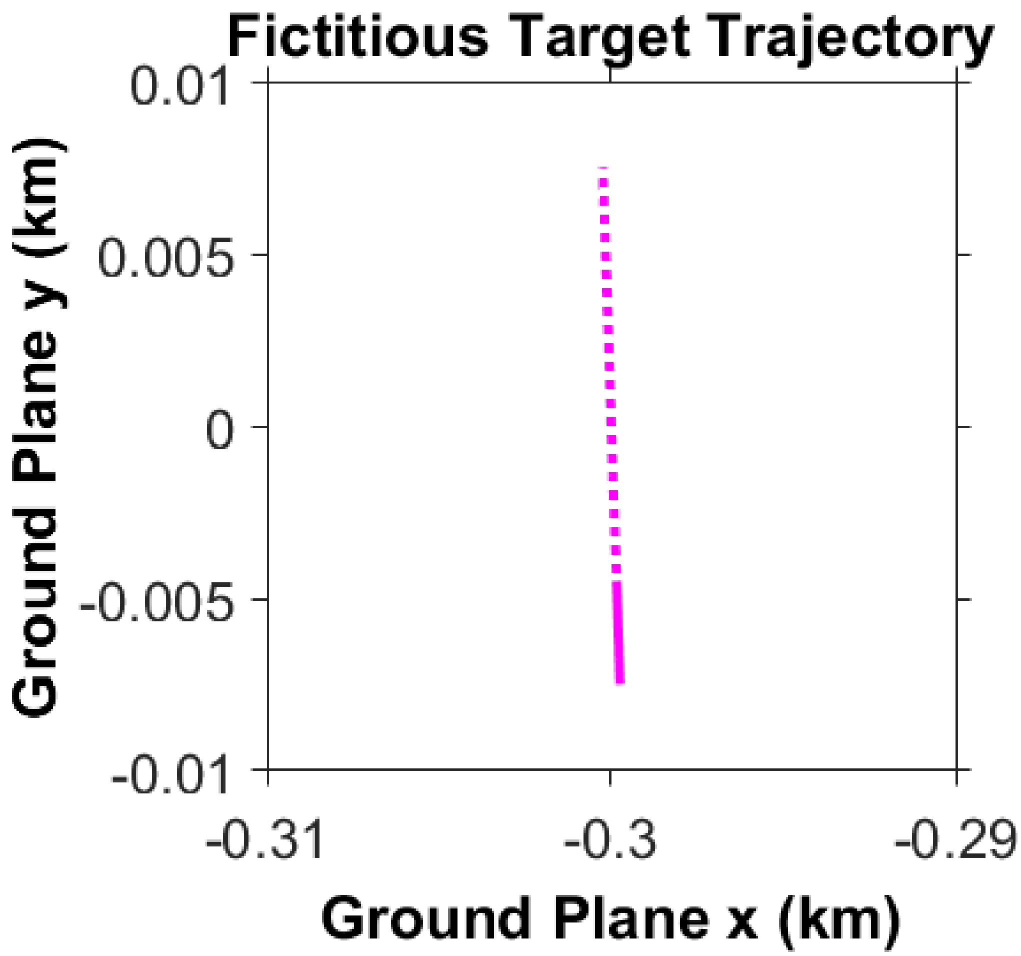


Figure 3. A zoomed image of the alternate fictitious target trajectory, wherein the initial 200 ms of the total 1000 ms corresponding to the full synthetic aperture is shown with a solid line, and the remainder is given by a dashed line. Thus, the alternate fictitious target is moving towards the radar in a direction which is approximately opposite to that of the true target motion.

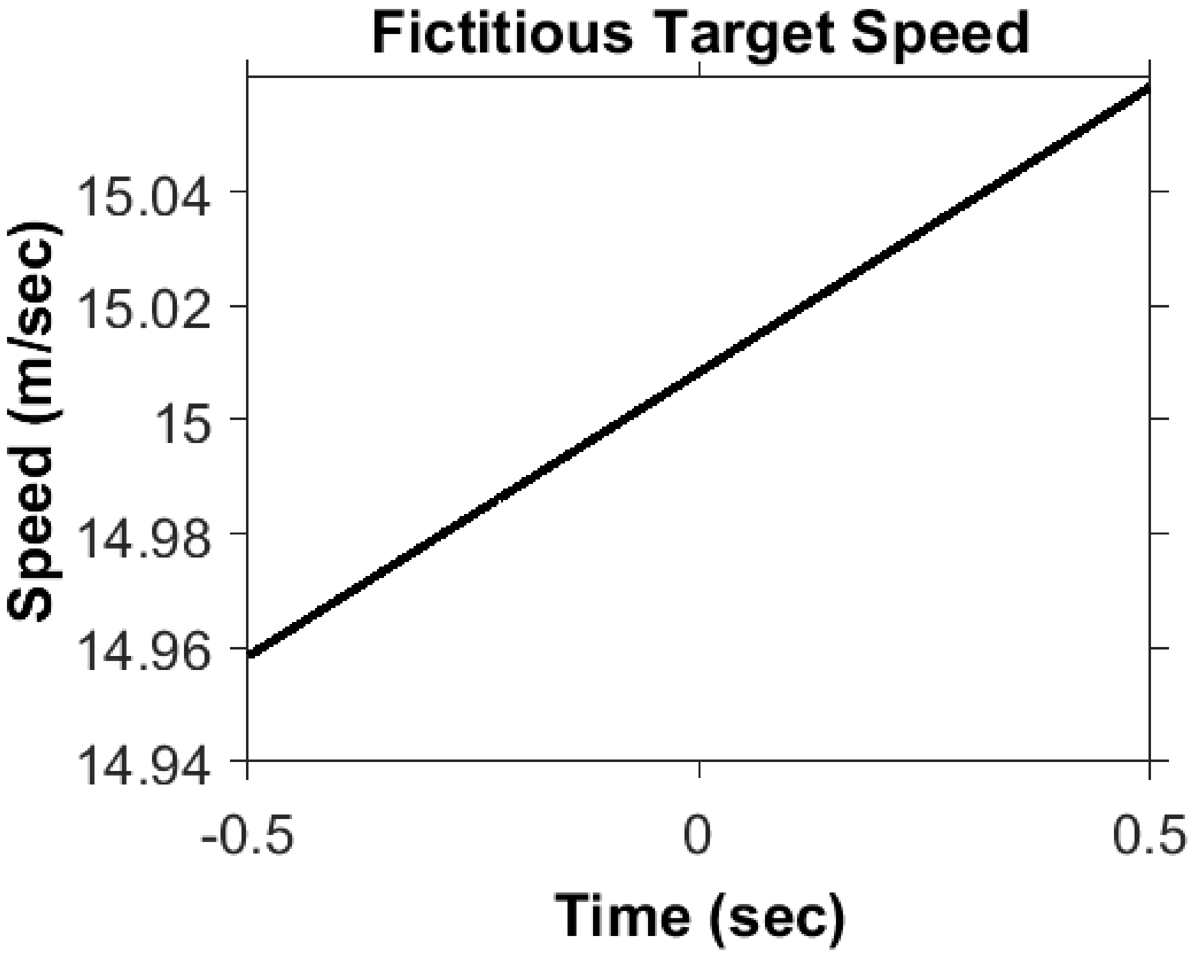


Figure 4. The ficititious target speed varies by approximately 1% over the SAR collection interval.

## ACKNOWLEDGMENTS

The author thanks AFRL for partial support of this work. DoD Distribution Statement A: Unlimited Distribution. The views expressed in this document are those of the author and do not reflect the official policy or position of the Department of Defense or the U.S. Government.

## REFERENCES

[1] Raney, R. K., "Synthetic aperture imaging radar and moving targets," *IEEE Transactions on Aerospace and Electronic Systems* **7**, pp. 499–505 (May 1971).

[2] Perry, R. P., DiPietro, R. C., and Fante, R. L., "SAR imaging of moving targets," *IEEE Transactions on Aerospace and Electronic Systems* **35**, pp. 188–200 (Jan 1999).

[3] Fienup, J. R., "Detecting moving targets in SAR imagery by focusing," *IEEE Transactions on Aerospace and Electronic Systems* **37**, 794–809 (Jul 2001).

[4] Cristallini, D., Pastina, D., Colone, F., and Lombardo, P., "Efficient detection and imaging of moving targets in SAR images based on chirp scaling," *IEEE Transactions on Geoscience and Reomote Sensing* **51**, 2403–2416 (Apr 2013).

[5] Jakowatz Jr., C. V., Wahl, D. E., and Eichel, P. H., "Refocus of constant velocity moving targets in synthetic aperture radar imagery," *Proc. SPIE: Algorithms for Synthetic Aperture Radar Imagery V, Edmund G. Zelnio, Editor.* **3370**, 85–95 (Apr 1998).

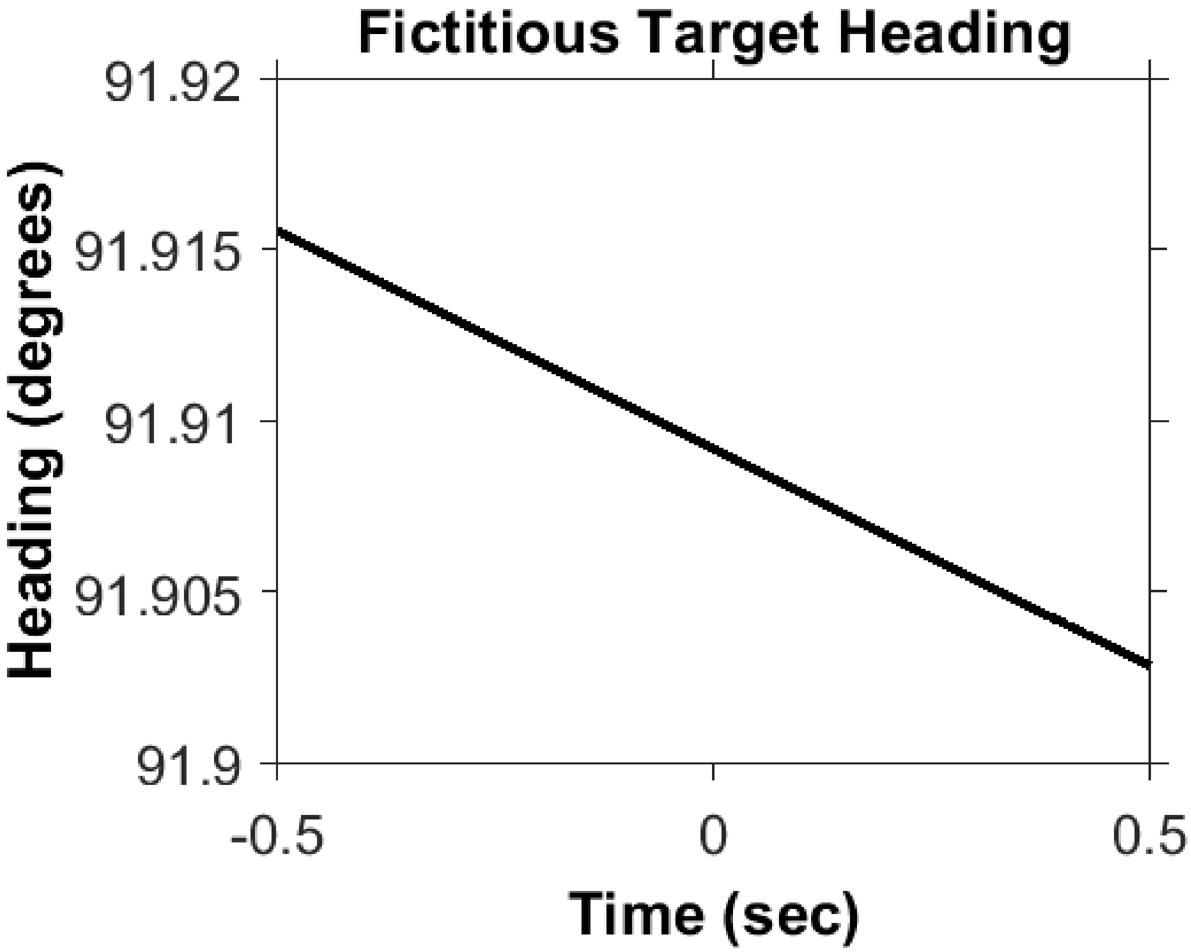


Figure 5. The ficititious target speed varies by less than 0.1° over the SAR collection interval.


[6] Rigling, B. D., "Image-quality focusing of rotating SAR targets," *IEEE Geoscience and Remote Sensing Letters* **5**, 750–754 (Oct 2008).

[7] Vu, V. T. S., Pettersson, T. K., Gustavsson, M. I., Ulander, A., and Lars, M. H., "Detection of moving targets by focusing in UWB SAR - theory and experimental results," *IEEE Transactions on Geoscience and Remote Sensing* **48**(10), 3799 (2010).

[8] Stojanovic, I. and Karl, W. C., "Imaging of moving targets with multi-static SAR using an overcomplete dictionary," *IEEE Journal of Selected Topics in Signal Processing* **4**, 164–176 (Feb 2010).

[9] Leducq, P., Ferro-Famil, L., and Pottier, E., "Matching-pursuit-based analysis of moving objects in polarimetric SAR images," *IEEE Geoscience and Remote Sensing Letters* **5**, 123–127 (Apr 2008).

[10] Fasih, A. R., Ertin, E., Ash, J. N., and Moses, R. L., "SAR focusing performance for moving objects with random motion components," *Signals, Systems and Computers, 2008. ACSSC 08. Forty-second Asilomar Conference on, Oct. 2008* , 1628–1632 (2008).

[11] Zhu, S., Liao, G., Qu, Y., Zhou, Z., and Liu, X., "Ground moving targets imaging algorithm for synthetic aperture radar," *IEEE Transactions of Geoscience and Remote Sensing* **49**, 462–477 (Jan 2011).

[12] Cheney, M. and Borden, B., "Waveform-diverse moving-target spotlight SAR," *Proceedings of the 2010 International Waveform Diversity and Design Conference held 8-13 August 2010 in Niagara Falls, Canada* , 33–34 (2010).

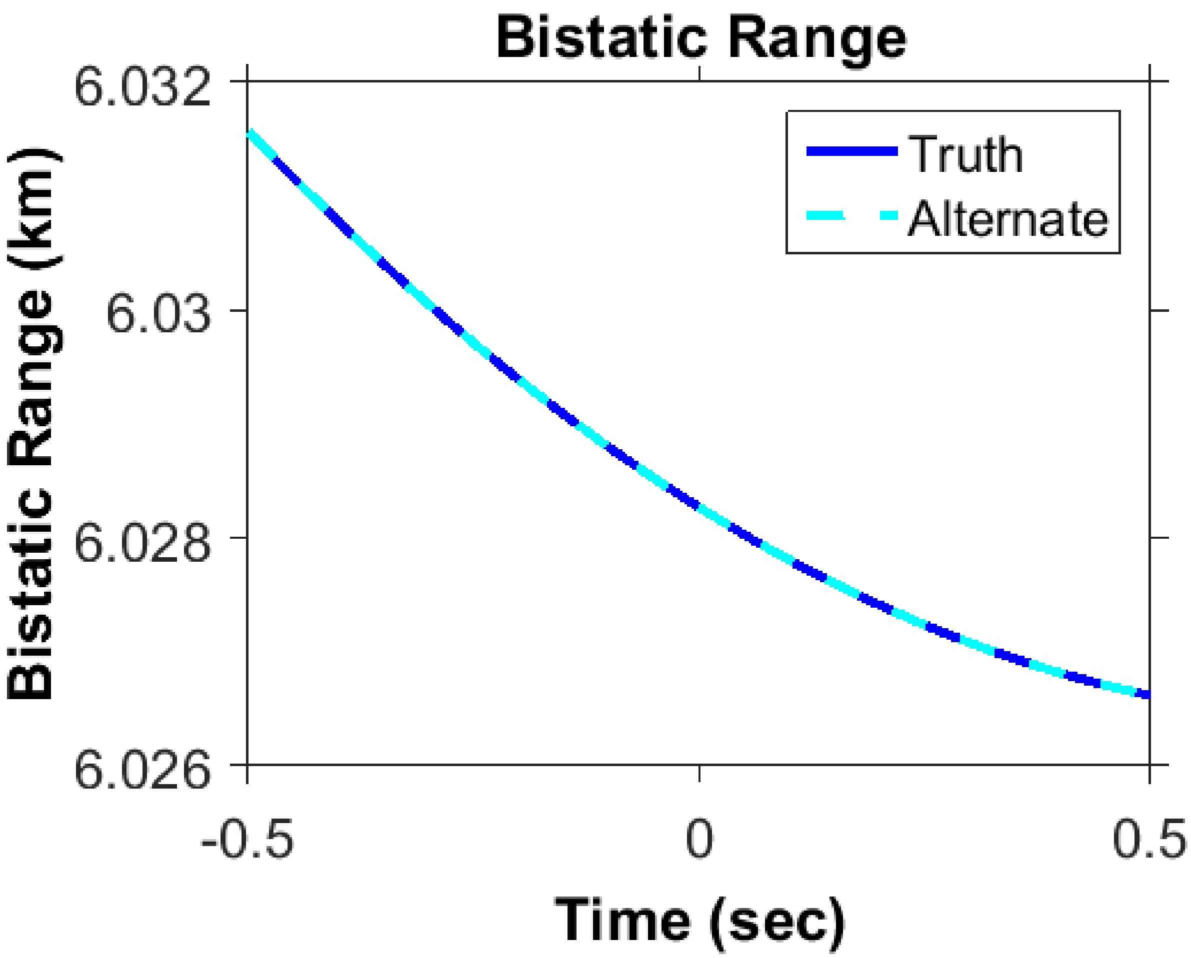


Figure 6. A comparison of the bistatic range values corresponding to the true target motion and that of the alternate fictitious target.

[13] Xu, J., Zuo, Y., Xia, B., Xia, X.-G., Peng, Y.-N., and Wang, Y.-L., "Ground moving target signal analysis in complex image domain for multichannel SAR," *IEEE Transactions on Geoscience and Remote Sensing* **50**, 538–552 (Feb 2012).

[14] Yake, L., Yanfei, W., and Chang, L., "Detect and autofocus the moving target by its range walk in time domain," *IEEE* (2011).

[15] Li, X., Deng, B., Qin, Y., Wang, H., and Li, Y., "The influence of target micromotion on SAR and GMTI," *IEEE Transactions on Geoscience and Remote Sensing* **49**, 2738–2751 (Jul 2011).

[16] Deng, B., Qin, Y., Wang, H., and Li, X., "An efficient mathematical description of range models for high-order-motion targets in synthetic aperture radar," *Proceedings of the 2012 IEEE Radar Conference held 7-11 May 2012 in Atlanta, Georgia* , 6–10 (2012).

[17] DiPietro, R. C., Fante, R. L., and Perry, R. P., "Space-based bistatic GMTI using low resolution SAR," *IEEE Aerospace Conference 1997* **2**, 181–193 (Feb 1997).

[18] Jao, J. K., "Theory of synthetic aperture radar imaging of a moving target," *IEEE Transactions on Geoscience and Remote Sensing* **39**, 1984 –1992 (Sep 2001).

[19] Garren, D. A., "Method and system for developing and using an image reconstruction algorithm for detecting and imaging moving targets - U.S. Patent 7456780 B1," (Nov 2008).

[20] Mao, X. Z. and Zhu, Z.-D. D.-Y., "Signatures of moving target in polar format spotlight SAR image," *Progress in Electromagnetics Research* **92**, 47–64 (2009).

[21] Mao, X., Zhu, D., Wang, L., and Zhu, Z., "Response of polar format algorithm to moving target with consideration of wavefront curvature," *2009 IEEE Radar Conference, Pasadena, CA* .

[22] Linnehan, R., Perlovsky, L., Mutz, C., and Schindler, J., "Detecting slow moving targets in SAR images," *Proceedings of SPIE 5410, Radar Sensor Technology VIII and Passive Millimeter-Wave Imaging Technology VII, 64 (August 12, 2004)* **64** (Aug 2004).

[23] Barbarossa, S. and Farina, A., "A novel procedure for detecting and focusing moving objects with SAR based on the Wigner-Ville distribution," *IEEE International Radar Conference* , 44 (1990).

[24] Barbarossa, S., "Detection and imaging of moving objects with synthetic aperture radar - Part 1: Optimal detection and parameter estimation theory," *IEE Proceedings-F* **139**, 79–88 (Feb 1992).

[25] Barbarossa, S. and Farina, A., "Detection and imaging of moving objects with synthetic aperture radar - Part 2: Joint time-frequency analysis by Wigner-Ville distribution," *IEE Proceedings-F* **139**, 89–97 (Feb 1992).

[26] Kirscht, M., "Detection and imaging of arbitrarily moving targets with single-channel SAR," *IEE Proceedings - Radar, Sonar, and Navigation* **150**, 7–11 (Feb 2003).

[27] Dias, J. M. B. and Marques, P. A. C., "Multiple moving target detection and trajectory estimation using a single SAR sensor," *IEEE Transactions on Aerospace and Electronic Systems* **39**, 604–624 (Apr 2003).

[28] Marques, P. A. C. and Dias, J. M. B., "Moving targets processing in SAR spatial domain," *IEEE Transactions on Aerospace and Electronic Systems* **43**, 864–874 (Jul 2007).

[29] Garren, D. A., "Smear signature morphology of surface targets with arbitrary motion in spotlight synthetic aperture radar imagery," *IET Radar, Sonar and Navigation* **8**, 435–448 (Jun 2014).

[30] Garren, D. A., "Signatures of braking surface targets in spotlight synthetic aperture radar," *Proceedings of 2014 Sensor Signal Processing for Defence, held in Edinburgh, UK, on 08-09 September 2014* , 51–55 (Sep 2014).

[31] Garren, D. A., "Signature predictions of surface targets undergoing turning maneuvers in spotlight synthetic aperture radar imagery," *Proceedings of SPIE, Vol. 9475, 94750A, Algorithms for Synthetic Aperture Radar Imagery XXII, 20 - 24 April 2015, in Baltimore, Maryland, USA* , 4997–5008 (Apr 2015).

[32] Garren, D. A., "Signatures of surface targets with increasing speed in spotlight synthetic aperture radar," *2015 IEEE International Radar Conference, 11-15 May 2015 in Arlington, Virginia, USA* , 1114 1118 (May 2015).

[33] Garren, D. A., "Theory of two-dimensional signature morphology for arbitrarily moving surface targets in squinted spotlight synthetic aperture radar," *IEEE Transactions on Geoscience and Remote Sensing* **53**, 4997–5008 (Sep 2015).

[34] Garren, D. A., "Signature morphology effects of squint angle for arbitrarily moving surface targets in spotlight synthetic aperture radar," *IEEE Transactions on Geoscience and Remote Sensing* **53**, 6241–6251 (Nov 2015).

[35] Duman, K. and Yazici, B., "Moving target artifacts in bistatic synthetic aperture radar images," *IEEE Transactions on Computational Imaging* **1**, 30–43 (Mar 2015).

[36] Minardi, M. J., Gorham, L. A., and Zelnio, E. G., "Ground moving target detection and tracking based on generalized sar processing and change detection," *Proceedings of SPIE, Vol. 5808, Algorithms for Synthetic Aperture Radar Imagery XII, 14 June 2005, in Orlando, FL, USA* **5808**, 156–165 (June 2005).

[37] Scarborough, S., Lemanski, C., Nichols, H., Owirka, G., Minardi, M., and Hale, T., "Sar change detection mti," *Proceedings of SPIE, Vol. 6237, Algorithms for Synthetic Aperture Radar Imagery XIII, 17 May 2006, in Orlando, FL, USA* **6237**, 62370V–1 – 62370V–11 (May 2006).

[38] Minardi, M. J. and Zelnio, E. G., "Comparison of sar based gmti and standard gmti in a dense target environment," *Proceedings of SPIE, Vol. 6237, Algorithms for Synthetic Aperture Radar Imagery XIII, 17 May 2006, in Orlando, FL, USA* **6237**, 62370X–1 – 62370X–10 (May 2006).

[39] Holston, M. E., Minardi, M. J., Temple, M. A., and Saville, M. A., "Characterizing geolocation ambiguity responses in synthetic aperture radar: ground moving target indication," *Proceedings of SPIE, Vol. 6568, Algorithms for Synthetic Aperture Radar Imagery XIV, 7 May 2007, in Orlando, FL, USA* **6568**, 656809 – 656809–11 (May 2007).

[40] Newstadt, G. E., Zelnio, E. G., Gorham, L., and III, A. O. H., "Detection/tracking of moving targets with synthetic aperture radars," *Proceedings of SPIE, Vol. 7699, Algorithms for Synthetic Aperture Radar Imagery XVII, 5 April 2010, in Orlando, FL, USA* **7699**, 7699DI–1 – 7699DI–10 (April 2010).

[41] Garren, D. A., "Ambiguities is target motion estimation for general SAR measurements," *IET Radar, Sonar and Navigation* **10**, 1720–1728 (Dec 2016).